SUPPLEMENTARY MATERIAL

Table 1

Statistic	OM-Rb^+	E71H-F103A (Closed state)
Data Collection		
Space group	I4	I4
Cell dimensions		
a=b, c (Å)	157.79, 73.88	156.14,76.29
$\alpha=\beta=\gamma$ (°)	90	90
Resolution (Å)	50-3.3	40-3.2
R_{merge} (%)	41.1	46.6
$I/\sigma I$	3.12	2(0.95)
Completeness	97.2	81.6
Redundancy	4.1	3.2(1.8)
Refinement		
No. reflections	13294	13994
R_{work}/R_{Free} (%)	24.04/25.6	21.95/26.95
No. atoms		
Protein	3923	3986
Ligand/ion	4	6
Water	--	--
B-factors		
Protein	112.123	52.75
Ligand/ion	118.54	84.19
Bond lengths (Å)	0.008	0.0074
Bond Angles (°)	1.44	1.44

*Highest resolution shell is shown in parenthesis

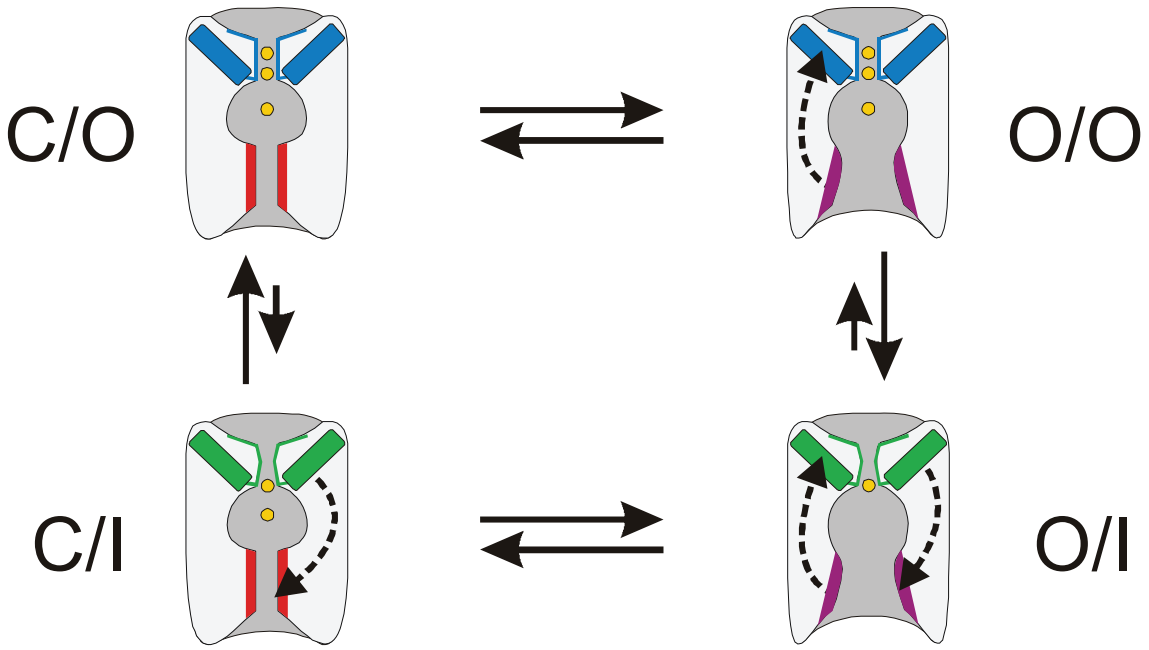

Figure S1. Conformational coupling between activation and inactivation gates in K^+ channels. A gating cycle is defined by four kinetic states, where the activation and selectivity filter gates exist in either conductive or non-conductive conformations. The two gates are coupled so that opening of the activation gates stabilizes the non-conductive conformation of the filter while inactivating the filter stabilizes the activation gate in its closed conformation.

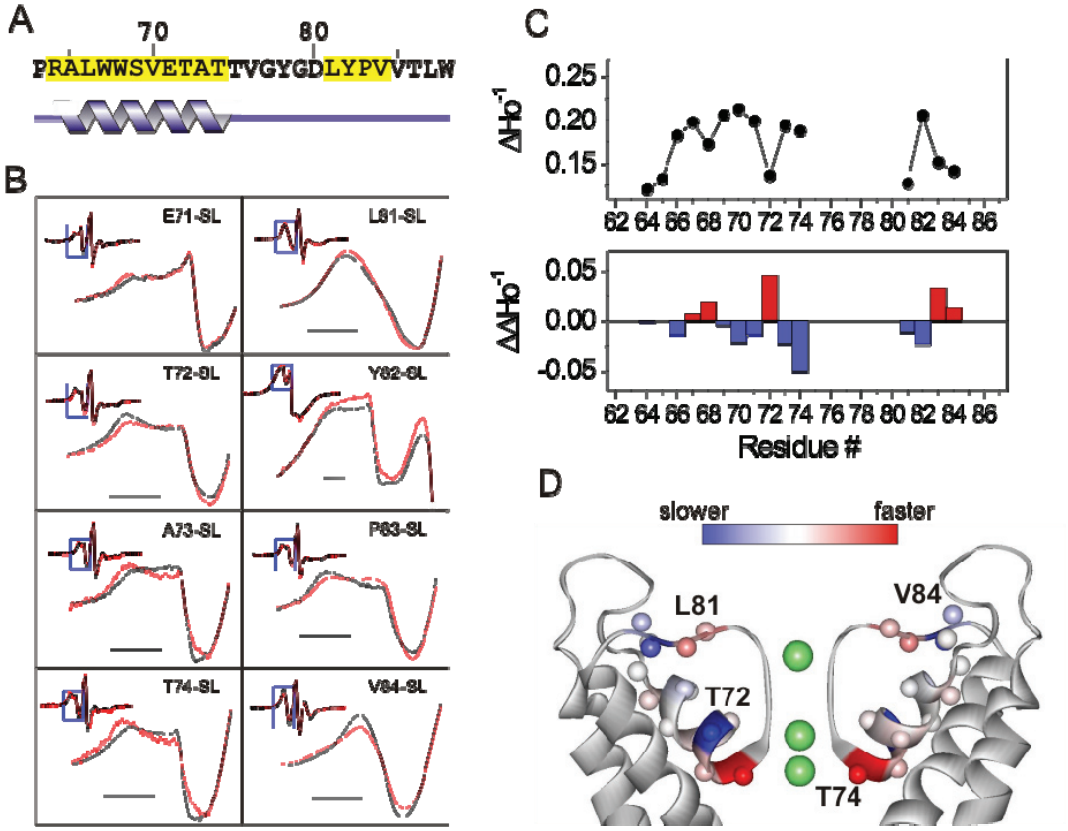

Figure S2. Activation gating is accompanied by subtle conformational changes near the selectivity filter. A. Amino acid sequence of the KcsA selectivity filter; shown in a yellow background are the spin labeled positions used for the present analysis. Secondary structure assignment according to the KcsA crystal structure appears in the bottom. B. pH-dependent changes in EPR spectral lineshape at selected residues flanking the signature sequence of the selectivity filter (shown for the low-field resonance line m = -1). Black traces correspond to spectra obtained at pH 7.0, red traces were obtained at pH 5.0. In each panel, the whole spectrum is shown as an inset. C. Nitroxide mobility (ΔHo^{-1}, top) mobility changes ($\Delta\Delta Ho^{-1}$, center) for spin-labeled pore mutants upon pH activation. In the bottom panel, increases in motional freedom are shown in red, decreases in motional freedom are shown in blue. In D, these data have been mapped onto the crystal structure according to the displayed color spectrum. For clarity, only two opposing subunits of KcsA are shown.

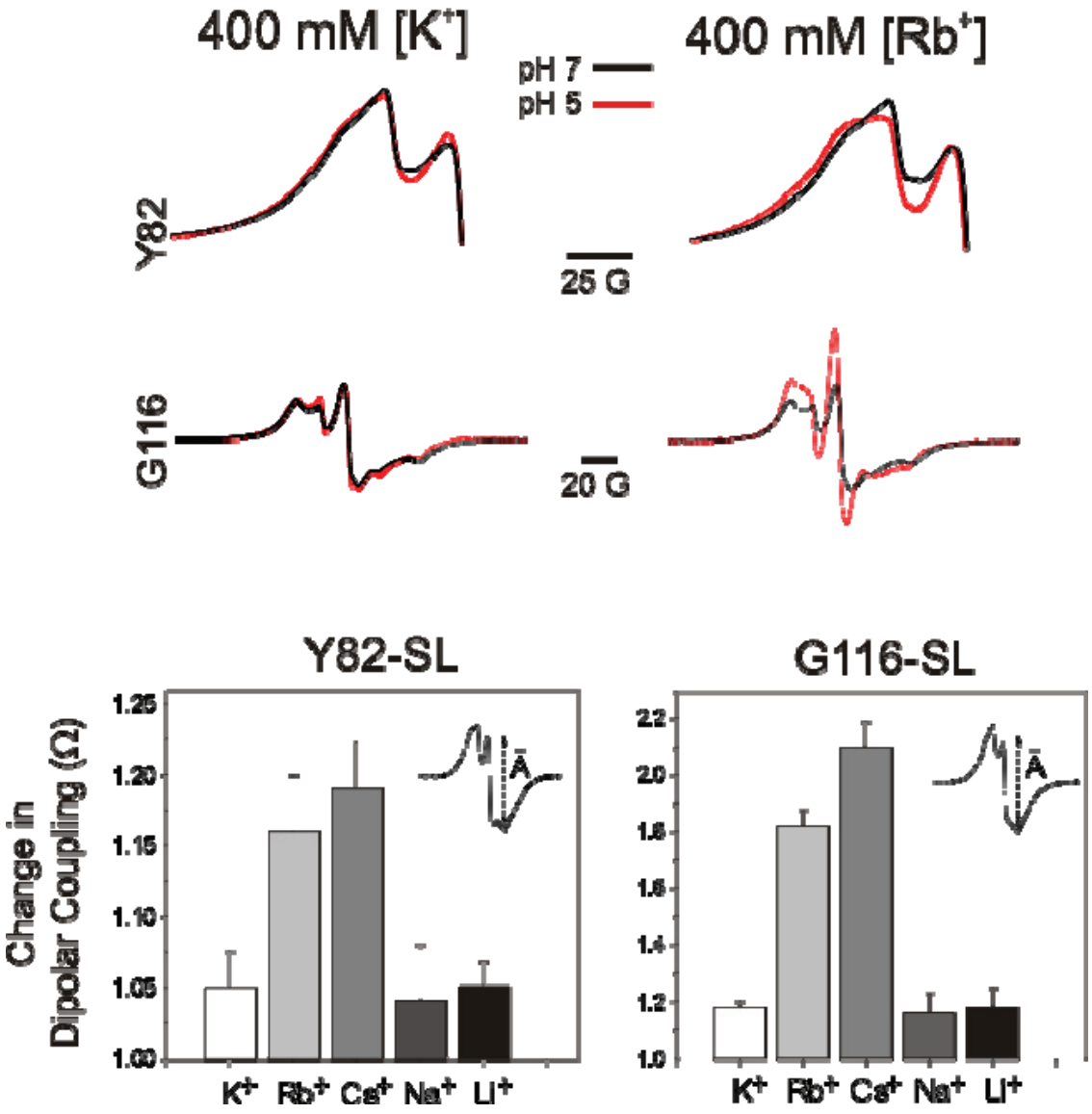

Figure S3. Top. CW-EPR spectra from positions near the selectivity filter (Y82) or the intracellular gate (G116). Black traces represent conditions favoring the closed state (pH 7), red traces report on the partially open state ensemble (pH 5). All data were obtained at high ionic strength (400 mM) but differ only on the type of permeant ion (K+ on the right set, Rb+ on the left). Spectra are shown normalized to the total number of spins in the sample. For residues near the selectivity filter, only the low field line (m = -1) is shown. Bottom. Magnitude of the conformational change, measured from the semi-quantitative dipolar coupling estimate (Ω parameter), for a series of monovalent cations. Results are reported for a position near the selectivity filter (Y82-SL, left) and at the intracellular gate (G116-SL, right).

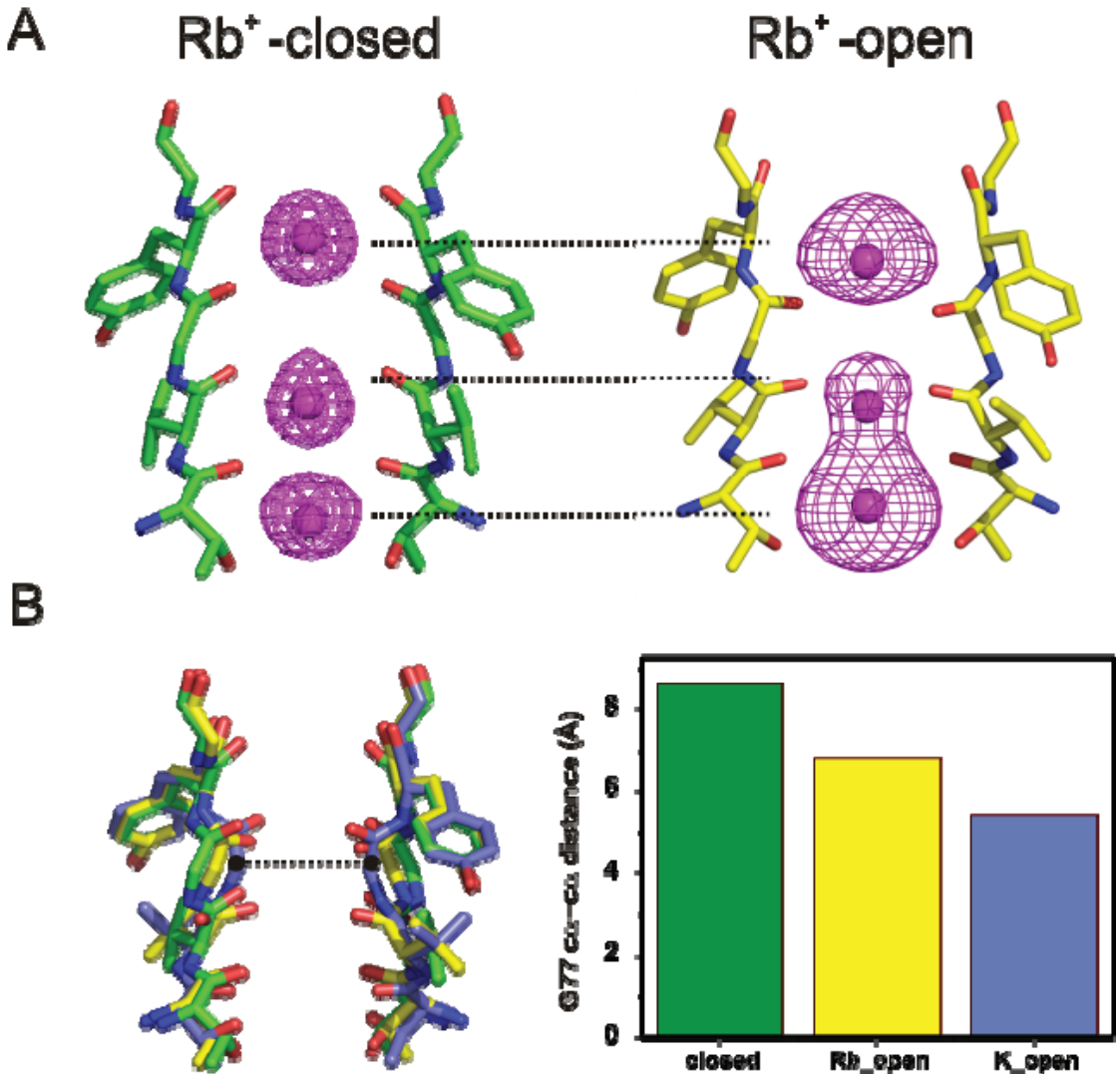

Figure S4. Structure of the selectivity filter in the presence of Rb^+ ions for the fully open KcsA leads only to a partially inactivated conformation. **a**. Fo–Fc omit map of Rb^+ ions in the selectivity filter with the filter backbone shown in stick representation in the closed (green) and fully open (yellow, 32 Å opening). The electron density maps are shown with 4σ contour for the closed state and 4σ for the open state. **b**. Selectivity filter structures overlapped for comparison: Closed gate conformation in K^+ (green), Open gate conformation in Rb^+ (yellow) and Open gate conformation in K^+ (blue). Right panel, Cα- Cα distance at Gly77 in each case.

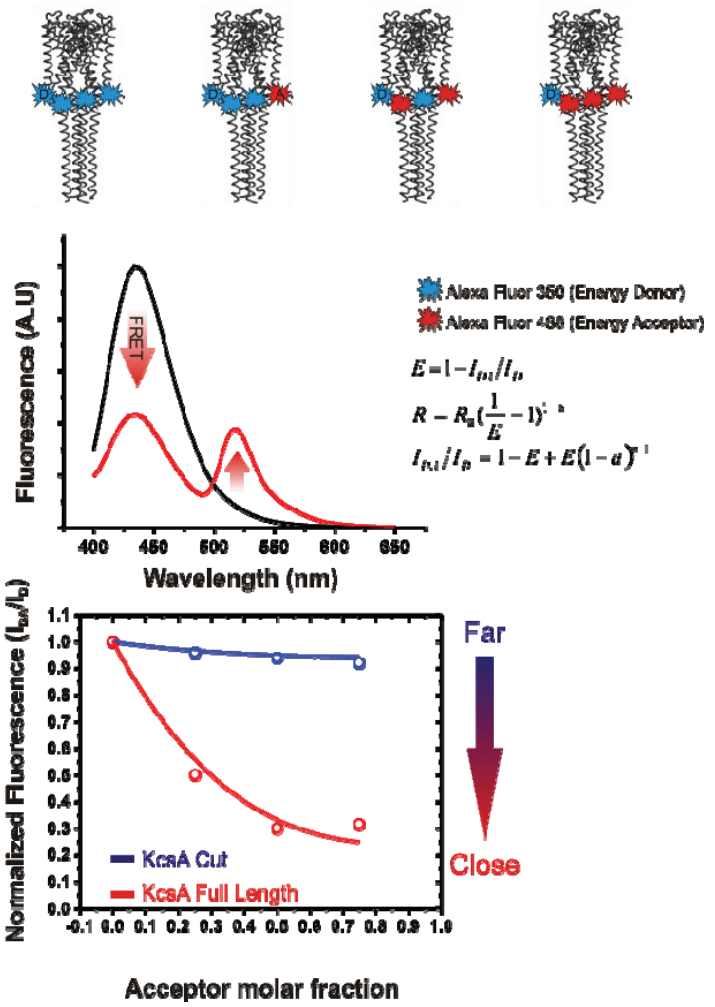

Figure S5. The extent of gate opening depends on the presence of the C-terminal domain in KcsA. Fluorescence energy transfer experiments using the dyes Alexa fluor 350 and 488 show that the FRET efficiency increases much more efficiently as a function of acceptor molar fraction in full-length KcsA, as compared with Chymotrypsin -truncated channels.

What are the consequences of deleting the C-terminus on the conformation of the inner gate? Fluorescence energy transfer experiments using pH insensitive probes Alexa Fluor 350 and Alexa Fluor 488 revealed that the energy transfer efficiency at the inner gate (G116C) decreases significantly after treatment with Chymotrypsin. This implies that the C-terminal truncation leads to a wider opening of the inner bundle gate than that of its full-length counterpart and that a physiologically relevant open KcsA structure is likely related not to the fully open state but to one of the “partially opened” structures described in our accompanying paper[7]. More importantly, this result implies that at least in KcsA, the coupling efficiency between gates appears to be proportional to the degree of opening in the inner helix bundle and reveals the underlying principle of conformational coupling from the gate to the filter.

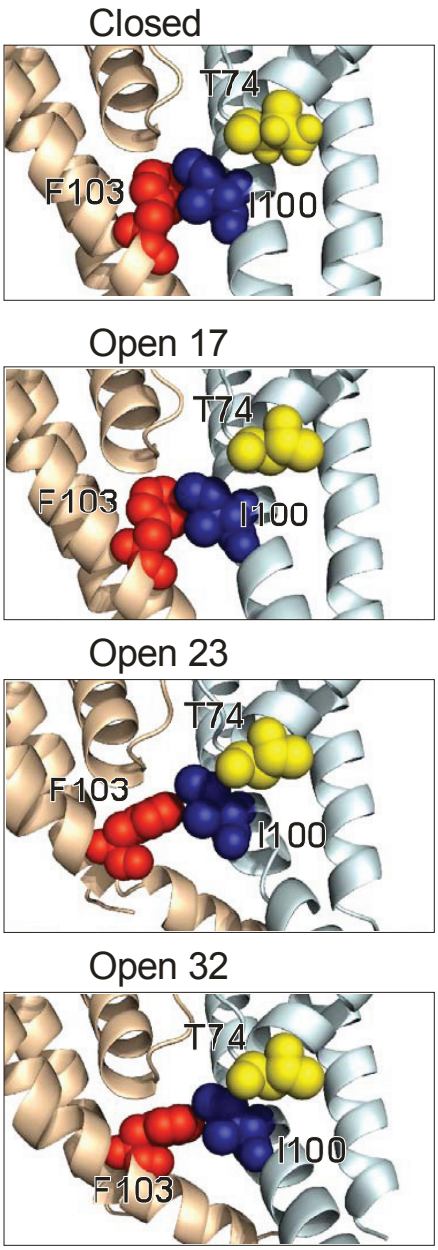

Figure S6. Conformational rearrangements in the KcsA aqueous cavity in a series of partially opened structures[7].Transmembrane helices are represented as ribbons, and residues Thr75, Ile100 and Phe103 are shown in space filling representation (vdW volumes).

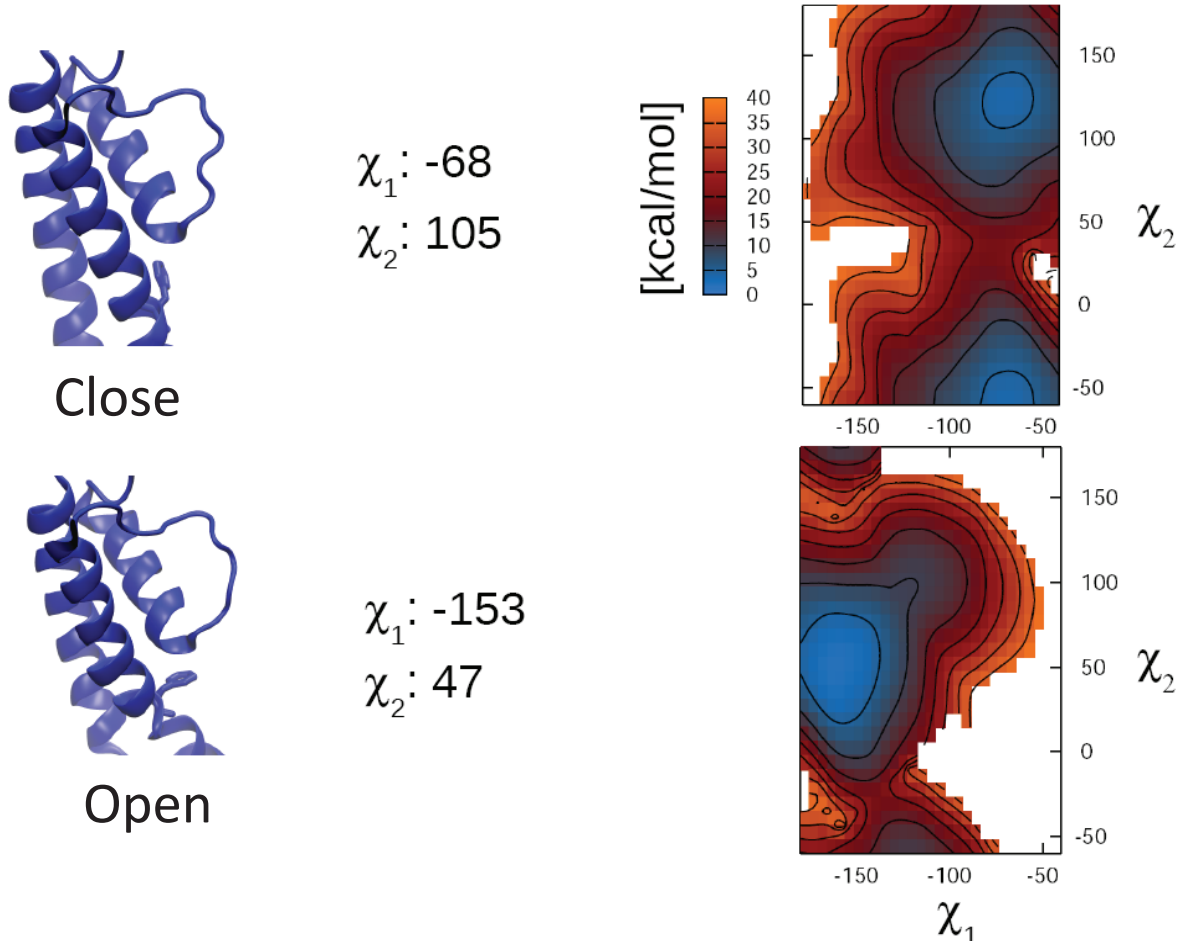

Figure S7. Side chain reorientation in F103 is forced by the opening of TM2. Adiabatic energy maps of the sidechain dihedral angles of F103 in the closed [top] and open (32 A) [bottom] states of KcsA. When the intracellular gate opens, the rotameric conformation of the Phe103 sidechain seen in the open inactivated crystal structure is highly favored compared to the preferred closed state conformation. This energetic balance suggests that the conformation of the Phe103 is a faithful reporter of the intracellular gate conformation and provides a possible mechanism for how information about the lower gate might be relayed to the selectivity filter. Contours are drawn every 5 kcal/mol.

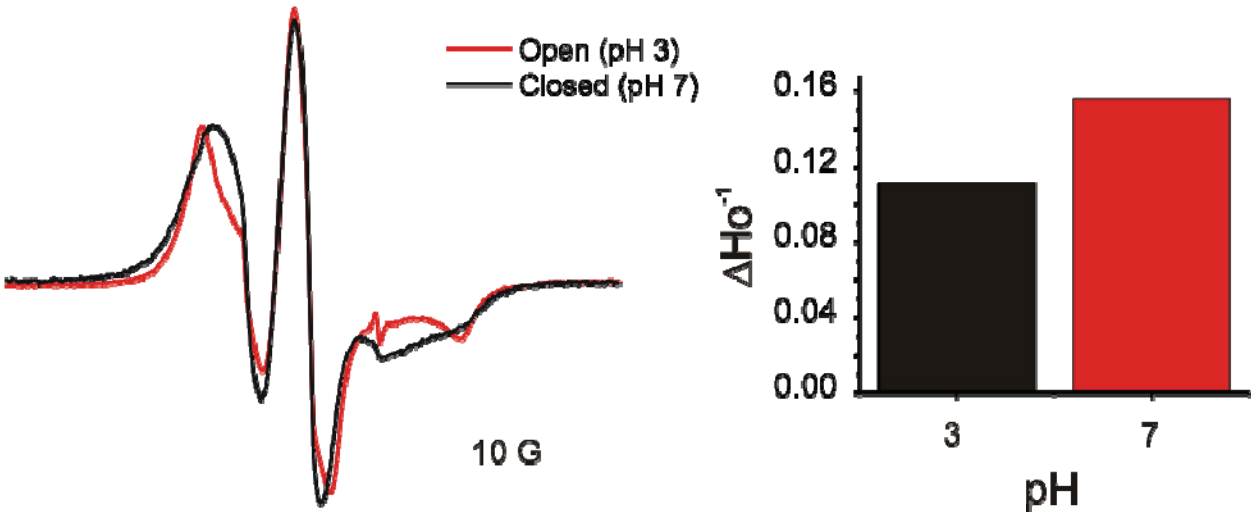

Figure S8. Conformational transitions at the internal aqueous cavity monitored at F103C. Upon channel opening a spin-label at position Phe103 shows a decrease in local dynamics with a simultaneous decrease in spin-spin dipolar coupling. This result is in agreement with the side chain rearrangements observed at the same position from crystal structures of partially and fully open KcsA.

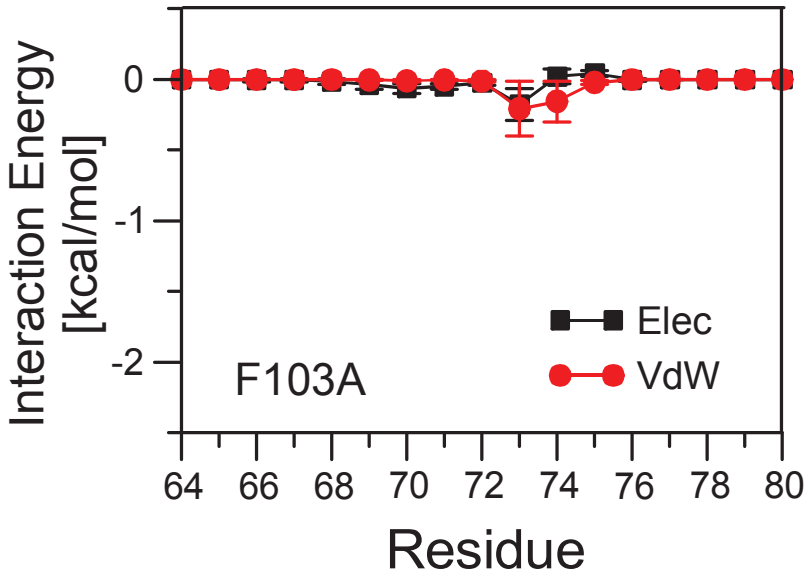

Figure S9. Average interaction energies between mutated Ala103 and side chains from residues in the pore helix calculated from MD runs of a full atom representation of the KcsA tetramer embedded in lipid. This is in contrast to the approximately 2 kcal/mol in VdW interaction energy between residues F103 and T74/T75.

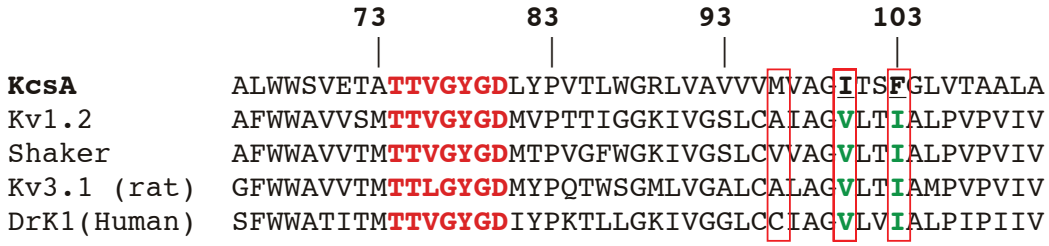

Figure S10. A common gate coupling mechanism in K^+ channels. Sequence alignment of the selectivity filter (signature sequence in red fonts) and pore helix for KcsA and representative members of the Kv channel superfamily. Residues aligning with position F103 in KcsA tend to be large volume/bulky side chains in Kv channels. These side chains might also participate in a steric interaction coupling between the inner bundle gate and the selectivity filter. Positions equivalent to residues M96, I100 and F103 (in KcsA) play important roles in C-type inactivation coupling (red bars).